InN-based optical waveguides developed by RF sputtering for all-optical applications at 1.55 μm

L. Monteagudo-Lerma, F.B. Naranjo, M. Jiménez-Rodríguez, P.A. Postigo, E. Barrios, P. Corredera, and M. González-Herráez

Abstract— **We report on the design, fabrication and optical characterization of InN-based optical waveguides aiming at their application as all-optical limiters at 1.55 μm. The InN guiding layers are grown by radio-frequency (RF) sputtering on sapphire substrates. Experimental cut-back method and nonlinear optical transmittance measurements were performed for the developed devices. The waveguides present nonlinear behavior associated with two photon absorption process. A nonlinear absorption coefficient ranging from ~43 cm/GW to ~114 cm/GW is estimated from optical measurements. These results open the possibility of using RF sputtering as a low cost and thermally harmless technique for the development and overgrowth of InN-based optical waveguides in future III-nitride all-optical integrated circuits working at telecom wavelengths.**

Index Terms— Indium nitride, sputtering, nonlinear optics, active waveguides, all-optical devices.

I. INTRODUCTION

Much effort is being made to introduce the all-optical approach in future telecommunication networks aiming at the fully exploitation of the extremely large bandwidth provided by optical fibers. For this purpose, new optical devices are required for performing active all-optical functions via different nonlinear optical processes at 1.55 μm. All-optical devices require highly nonlinear materials with ultrafast response while presenting the highest transmittance change with the lowest control pulse energy. In particular, all-optical switching has been demonstrated by several heterostructures on GaAs [1] and InP [2] substrate platforms presenting relaxation times in the range of few picoseconds. III-nitride semiconductors emerged as attractive materials for all-optical signal processing at 1.55 μm through the enhanced third-order nonlinearity due to the asymmetry of their crystalline structure. Among them, quantum wells (QWs) and quantum dots (QDs) based on GaN/AlN heterostructures can efficiently perform this function via intersubband transitions with ultrafast relaxation times in the range of 150-400 fs [3,4] for the TM polarization of light at 1.55 μm. Apart from these heterostructures, the interband transition of InN/InGaN systems with relaxation lifetimes of a few ps [5] can be considered as an interesting active alternative for covering the telecommunications C-band (1.53-1.57 μm). Another option comes from the InN material with band gap energy ~0.7 eV [6] which operates at 1.55 μm presenting recovery times in the range of ps [7]. Finally, InN material by radio-frequency (RF) sputtering with the band gap at ~1.7 eV provides an attractive solution for two-photon-absorption (TPA) based limiters devices, showing recovery times in the range of 300 fs [8].

On the other hand, photonic integrated circuits (PICs) are rapidly being developed due to their versatility to include several optical functions in a tiny space while consuming low power. III-nitrides are very promising materials for implementation in PICs for all-optical communication applications at 1.55 μm. Low control switching energies below 38 pJ for 10 dB of transmittance contrast have been reported for optical waveguides based on GaN/AlN QWs and QDs heterostructures grown on *c*-sapphire substrates [9,10]. Hence, considering these results, in this letter we focus on the development of novel InN-based optical waveguides for all-optical limitation applications at 1.55 μm. The InN guiding layer was deposited by RF sputtering on *c*-sapphire taking advantage of its lower refractive index compared to those of III-nitrides which enables good waveguiding while avoiding the light absorption by the substrate due to its high transparency at telecom wavelength. Sputtering takes profit of being a low cost technique while enabling the layers overgrowth at relatively low temperatures avoiding the likely material damage induced by high temperature processes.

II. EXPERIMENTAL

Two different InN guiding layers are considered for the fabrication of the optical devices: (1) a columnar InN film deposited on sapphire using an AlN buffer layer and (2) a compact InN layer grown directly on sapphire. Optical design of the waveguides was performed via the commercial mode solver RSoft BeamProp aiming at reaching single mode propagation by taking into account the refractive index contrast and the waveguide geometry. The considered refractive indices of sapphire, InN and AlN materials at 1.55 μm are 1.740, 2.280 and 2.125, respectively.

L. Monteagudo-Lerma, F.B. Naranjo, M. Jiménez-Rodríguez, and M. González-Herráez are with the Grupo de Ingeniería Fotónica, Departamento de Electrónica, Universidad de Alcalá, Madrid, 28871 Alcalá de Henares, Spain (e-mail: laura.monteagudo@depeca.uah.es; naranjo@depeca.uah.es; marco.jimenez@depeca.uah.es; miguelg@depeca.uah.es).

P.A. Postigo is with the Instituto de Microelectrónica de Madrid, 28760 Tres Cantos, Madrid, Spain (e-mail: pabloaitor.postigo@imm.cnm.csic.es).

E. Barrios was with the Instituto de Ciencia de Materiales de Madrid, 28049 Madrid, Spain (e-mail: ebarriosdiaz87@gmail.com).

P. Corredera is with the Instituto de Óptica, CSIC, Serrano 121, 28006 Madrid, Spain (e-mail: pcorredera@ifa.cetef.csic.es).

The columnar InN layer was grown on a double 60-nm-thick AlN buffer layer. The synthesis of the buffer was carried out following a previously optimized two-step deposition method [11]. The InN layer deposition was performed at 40 W of RF power, 450 °C of substrate temperature, 3.5 mTorr of sputtering pressure and pure nitrogen (6N) atmosphere. This InN guiding layer presents a columnar morphology with a diameter of the nanocolumns estimated by atomic force microscopy, of ~87 nm [12]. Optical simulations of the waveguide structure based on this columnar layer lead to an optimized thickness of the InN guiding layer of ~600 nm to ensure modal guiding at 1.55 µm for the minimum ridge width under study (2 µm). These values of thickness and minimum waveguide width are similar to those of the developed GaN/AlN-based waveguides [10] enabling an improved light coupling between both devices within a III-nitride-based PIC. In a second step, the etching depth is investigated considering values from 50 nm to 600 nm for the 2-µm-wide and 2-mm-long columnar waveguide in order to accomplish single mode propagation while minimizing the modal guiding through the slab. Following these simulations, single mode behavior is expected for etching depths from 50 nm to 200 nm whereas multimode propagation is obtained for ridge heights larger than 250 nm. Among the required values for single mode propagation, the optimized etching depth was 100 nm since it leads to the highest confinement of light through the waveguide while presenting the lowest theoretical effective mode area of ~1.6 µm^2.

The second investigated InN guiding layer is a 350-nm-thick compact InN layer grown directly on sapphire substrate at lower temperature than the columnar film (300 °C) but keeping constant the rest of the deposition parameters. Optical design of the compact InN-based waveguide is also investigated in order to optimize the ridge dimensions for single mode propagation. Considering a ridge width of 2 µm, etching depths varying from 50 nm to 350 nm are investigated. The best result is obtained for 350 nm etching depth since it induces single mode propagation while presenting the lowest effective area of ~0.9 µm^2 within the analyzed range of ridge heights. Furthermore, it presents the easiest technological process since it is only required to etch down to the substrate.
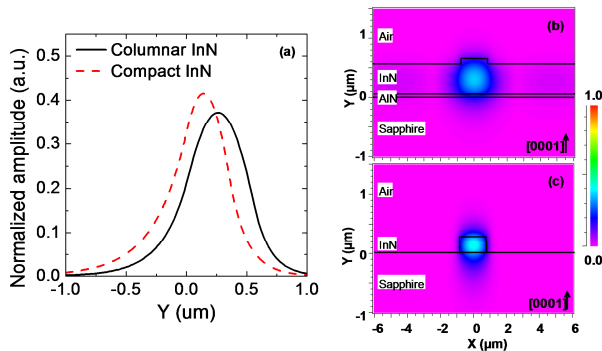

Fig. 1. (a) Normalized modal amplitude profile obtained at the output of both InN-based waveguides. Normalized modal amplitude maps for (b) the columnar InN waveguide and (c) the compact InN one.

Fig. 1(a) shows the modal amplitude profile at the output of the two optimized InN-based devices together with their corresponding modal amplitude color maps [see Fig. 1(b) and

Fig. 1(c)]. In all cases, the modal amplitude has been normalized with respect to the power of the field launched into the device. Under the consideration that both InN materials present a similar nonlinear absorption coefficient, an enhanced nonlinear response should be expected for the waveguide based on the compact InN layer as it shows a better modal confinement through the waveguide (lower effective mode area) and higher normalized maximum modal amplitude of 42% compared to that of the columnar InN waveguide of 37% [see Fig. 1(a)].

The 600-nm-thick columnar InN film shows an apparent optical band gap of ~1.69 eV with an absorption band edge of ΔE~0.174 eV [12]. On the other hand, the 350-nm-thick compact InN film presents a band gap energy of ~1.77 eV with ΔE~0.133 eV. The large band gap value obtained for both InN layers is associated with the Burstein-Moss effect due to the high residual carrier concentration, in the range of 10^{20} cm^{-3} [8]. Furthermore, both layers present wurtzite structure with a FWHM of the rocking curve around the InN(0002), of 2.7° and 2.2° for the columnar and the compact InN layers, respectively. In addition, the investigated InN layers show similar rms surface roughness, estimated by AFM measurements, of ~6 nm. Field-emission scanning electron microscopy (FESEM) images of these columnar and compact InN films are shown in Fig. 2(a) and Fig. 2(b), respectively.
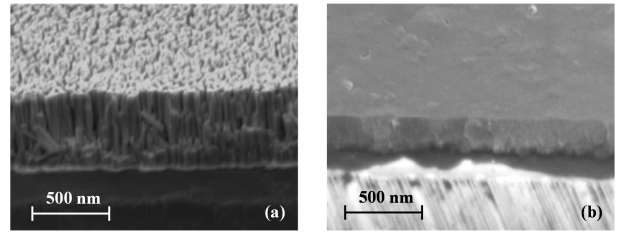

Fig. 2. FESEM images of (a) the columnar InN layer deposited on sapphire by using a double AlN buffer and (b) the compact InN layer deposited directly on sapphire.

The devices processing consists of three main steps. First of all, the patterning of the guiding structures is carried out by UV lithography considering waveguides width of ~2 µm. Afterwards, these InN-based layers are etched by physical RF sputtering at room temperature by using pure Ar (5N) plasma with 40 W of RF power applied to the substrate at a chamber pressure of 3.5 mTorr. Finally, the fabrication process entails the mechanical polishing of the waveguide facets.

III. RESULTS AND DISCUSSION

Optical characterization of the waveguides was performed at linear and nonlinear regimes using a mode-locked fiber laser operating at 1.55 µm with a pulse width of 100 fs and a repetition rate of 100 MHz. The laser output was coupled into an optical fiber and split using an optical fiber coupler (99/1); 99% of the signal was used to perform the linear and nonlinear measurements and the rest was used as a signal power reference. Light was controlled in polarization and coupled into the waveguides by means of a ~2.5-µm-diameter-spot lensed fiber. The pulse is broadened by the whole optical system up to 150 fs. Besides, the waveguide is mounted on a

3-axis positioning stage with tilt and rotation controls. The light at the output of the device was collected by a second lensed fiber similar to that used at the input facet of the device. The collected light is driven to a power meter in order to measure the output optical power at 1.55 µm.

Fig. 3 shows the results of the cut-back experiments [13] for both columnar and compact waveguides for TE and TM light polarization under incident power conditions (-2 dBm input average power) that ensure negligible non-linear behavior of the devices at 1.55 µm. It has to be pointed out that electric field of light is considered to vibrate along the growth direction for the TM polarization and perpendicular for the TE one. The difference in coupling and propagation losses between TE- and TM-polarizations is almost negligible for both types of waveguide. The vanishing of the polarization dependence of the transmittance due to the geometrical asymmetry of the waveguides is attributed to enhanced Rayleigh scattering in waveguide sidewalls defined by the sputtering etching.
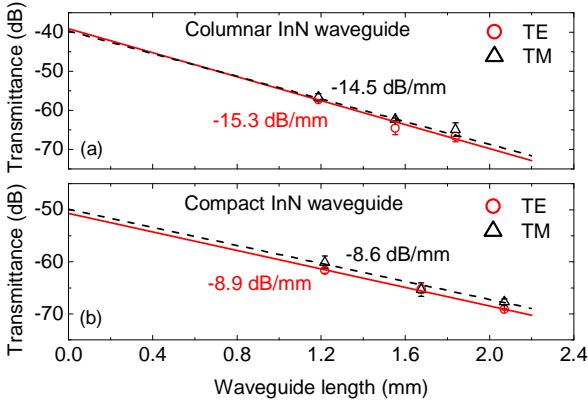

Fig. 3. Experimental cut-back method performed for TE and TM light at low incident optical power (-2 dBm) for (a) the columnar InN waveguide and (b) the compact InN one.

Particularly, coupling losses in the compact InN waveguide are much larger (~50 dB) than those in the columnar one (~40 dB). This difference can be related to the waveguide geometry since the columnar InN waveguide has an InN guiding layer quite thicker (600 nm) than the compact one (350 nm) maintaining both the same ridge width (2 µm). Considering the propagation losses, they are much higher for the columnar InN waveguide (~15 dB/mm) compared to those corresponding to the compact InN device (~8.7 dB/mm). Thus, the difference in propagation losses between both devices can be mainly attributed to the better confinement of the optical mode through the compact InN waveguide reducing the light diffraction along the x-axis while minimizing the optical losses due to surface roughness at the involved interfaces. Furthermore, the nanocolumns forming the columnar InN waveguide could act as internal scattering centers leading to a larger contribution of optical loss due to Rayleigh scattering effects compared to the compact InN waveguide. Also the nanostructured morphology of the columnar InN device could imply a reduction of the effective refractive index of the InN material. This could induce a lowering of the optical confinement of the light due to the reduction of the refractive index contrast within the structure.

It has to be noticed that in the following transmittance measurements performed in isolated optical waveguides, the coupling losses have been considered equally distributed between both facets.

Fig. 4 shows the experimental transmittance for both InN-based devices as a function of the input pulse energy together with FESEM images of (a) the plane view of the 2-µm-wide and 100-nm-deep columnar InN waveguide and (b) the cross section of the 2-µm-wide and 350-nm-deep compact InN waveguide. A reduction of the transmittance from low to high input pulse energies is clearly observed reaching a maximum contrast in both devices of ~6 dB for TE light and ~4.5 dB for TM polarization. The observed reverse saturable absorption is attributed to a TPA process that shows polarization dependence due to the asymmetry of the InN crystals.
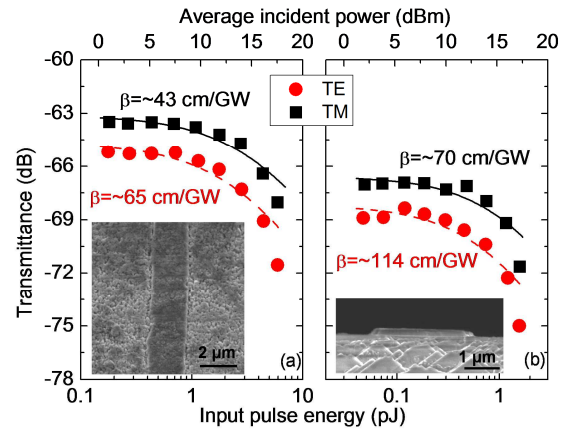

Fig. 4. Experimental transmittance for TE and TM light as a function of the input pulse energy together with the fitting curve by Eq. (1) for (a) the 1.8-mm-long columnar InN waveguide and (b) the 2.1-mm-long compact InN waveguide. Insets: FESEM images of (a) the top view of the columnar InN waveguide and (b) the cross section of the compact InN device.

The generalized Lambert-Beer's Law including the nonlinear absorption contribution through TPA process is given by $\frac{dI}{dz} = -\alpha_0 I - \beta I^2$, being α_0 and β the linear and nonlinear absorption coefficients, respectively. When integrating this equation along the whole length of the waveguide (L), the optical transmittance through a waveguide as a function of the input pulse energy (E_{pulse}) is given by:

$$T_{TPA} = \frac{e^{-\alpha_0 L}}{1 + \beta \frac{L_{eff}}{A_{eff} \cdot \Delta t} E_{pulse}} \qquad (1)$$

where A_{eff} is the effective mode area, L_{eff} is the effective length of the device and Δt is the temporal pulse width entering the optical waveguide. By fitting the experimental results from Fig. 4 to Eq. (1), both linear and nonlinear absorption coefficients can be estimated (see Table I).

In all cases, the transmittance obtained for the maximum input power significantly differs from the calculated expected value from data fitting to Eq. (1). This increased absorption at the highest input pulse intensity analyzed (~2.7 GW/cm²) could be attributed to a likely contribution of nonlinear free carrier absorption (FCA) effect by the free electrons excited

by the TPA process. This FCA phenomenon is enhanced at high optical intensities following a cubic dependence on the input power [14]. The values of β estimated at 1.55 µm in this work (see Table I) are larger for TE-light than for TM-light in both devices. The ratios between both polarization-dependent β values are estimated to be ~1.5 and ~1.6, for the columnar waveguide and the compact InN one, respectively. This polarization-dependent response is due to the crystal asymmetry of the wurtzite InN material. TE-light pumps the sample directly onto the basal crystallographic plane of the InN hexagons, exciting only one component of the third-order susceptibility tensor responsible of the nonlinear TPA ($\chi_{xxxx}^{(3)}$, because of the isotropy of the basal plane). However, TM-light excites the component along the c-axis ($\chi_{zzzz}^{(3)}$) since the electric field vibrates along the hexagon axis [15].

TABLE I
OPTICAL PARAMETERS OBTAINED FOR BOTH InN WAVEGUIDES

	Columnar InN waveguide		Compact InN waveguide	
	TM	TE	TM	TE
α_0 (cm^{-1})	80.7±0.2	82.7±0.3	74.1±0.3	75.9±0.3
L_{eff} (mm)	0.12	0.12	0.14	0.13
β (cm/GW)	43.4±8.3	65.2±14.0	69.6±18.7	113.6±30.6
E_{pulse} for 3 dB contrast (pJ)	4.6	3.6	1.3	1.1

In addition, it has to be highlighted that the obtained values of β are larger than that reported for InP with a recovery time in the subpicoseconds range [16], and those of Si(111) and GaAs, of 0.88 cm/GW and 10.2 cm/GW, respectively [17]. Nevertheless, the nonlinear absorption coefficients estimated from these InN-based devices are lower than the obtained in sputtered-bulk InN in our group (167±30 cm/GW) [8]. It should be noticed that this value corresponds to TE-light excitation in the transmittance measurements of the waveguides. Thus, the lower value of β estimated from measurements in waveguides could be attributed to a slight underestimation of the coupling losses in both studied devices.

The efficiency of the developed InN-based waveguides as nonlinear optical devices is assessed by considering the 3 dB of optical loss increase as the figure of merit. The input pulse energies required for reaching a 3-dB change for TE- and TM-light for both devices are presented in Table I. The best result is obtained for the compact InN-based device, with a value of input pulse energy to achieve a 3-dB transmittance contrast of ~1 pJ. This value is similar to the values required in more complex GaN/AlN-quantum-based waveguides showing saturable absorption, it being 3 pJ of input pulse energy [10].

IV. CONCLUSION

The capability of sputtered-InN-based optical waveguides to act as high-efficient reverse saturable absorbers via the TPA process has been demonstrated. The obtained results open the possibility of using RF sputtering as a low cost deposition technique for the development of InN-based optical waveguides in a thermally harmless procedure. These InN-based devices could act as all-optical limiters within a III-nitride-based PIC at 1.55 µm.

REFERENCES

[1] C. Husko, A. De Rossi, S. Combrié, Q.V. Tran, F. Raineri, and C.W. Wong, "Ultrafast all-optical modulation in GaAs photonic crystal cavities", *Appl. Phys. Lett.* vol. 94, no. 2, pp. 021111/1–3, 2009.

[2] A.V. Gopal, H. Yoshida, A. Neogi, N. Georgiev, T. Mozume, T. Simoyama, O. Wada, and H. Ishikawa, "Intersubband absorption saturation in InGaAs–AlAsSb quantum wells", *IEEE J. Quantum Elect.* vol. 38, no. 11, pp. 1515–1520, 2002.

[3] J. Hamazaki, S. Matsui, H. Kunugita, and K. Ema, "Ultrafast intersubband relaxation and nonlinear susceptibility at 1.55 µm in GaN/AlN multiple-quantum wells", *Appl. Phys. Lett.* vol. 84, no. 7, pp. 1102–1104, 2004.

[4] S. Valdueza-Felip, F.B. Naranjo, M. González-Herráez, H. Fernández, J. Solis, F. Guillot, E. Monroy, L. Nevou, M. Tchernycheva, and F.H. Julien, "Characterization of the resonant third-order nonlinear susceptibility of Si-doped GaN/AlN quantum wells and quantum dots at 1.5 µm", *IEEE Photon. Technol. Lett.* vol. 20, no. 16, pp. 1366–1368, 2008.

[5] F.B. Naranjo, M. González-Herráez, H. Fernández, J. Solís, and E. Monroy, "Third order nonlinear susceptibility of InN at near band-gap wavelengths", *Appl. Phys. Lett.* vol. 90, no. 9, pp. 091903/1–3, 2007.

[6] A.G. Bhuiyan, A. Hashimoto, and A. Yamamoto, "Indium nitride (InN): A review on growth, characterization and properties", *J. Appl. Phys.* vol. 94, no. 5, pp. 2779–2808, 2003.

[7] F.B. Naranjo, P.K. Kandaswamy, S. Valdueza-Felip, V. Calvo, M. González-Herráez, S. Martín-López, P. Corredera, J.A. Méndez, G.R. Mutta, B. Lacroix, P. Ruterana, and E. Monroy, "Nonlinear absorption of InN/InGaN multiple-quantum-well structures at optical telecommunication wavelengths", *Appl. Phys. Lett.* vol. 98, vol. 3, pp. 031902/1–3, 2011.

[8] S. Valdueza-Felip, L. Monteagudo-Lerma, J. Mangeney, M. González-Herráez, F.H. Julien, and F.B. Naranjo, "Nonlinear absorption at optical telecommunication wavelengths of InN films deposited by RF sputtering", *IEEE Photon. Technol. Lett.* vol. 24, no. 22, pp. 1998–2000, 2012.

[9] Y. Li, A. Bhattacharyya, C. Thomidis, T.D. Moustakas, and R. Paiella, "Ultrafast all-optical switching with low saturation energy via intersubband transitions in GaN/AlN quantum-well waveguides", *Opt. Express* vol. 15, no. 26, pp. 17922–17927, 2007.

[10] L. Monteagudo-Lerma, S. Valdueza-Felip, F.B. Naranjo, P. Corredera, L. Rapenne, E. Sarigiannidou, G. Strasser, E. Monroy, and M. González-Herráez, "Waveguide saturable absorbers at 1.55 µm based on intraband transitions in GaN/AlN QDs", *Opt. Express* vol. 21, no. 23, pp. 27578–27586, 2013.

[11] L. Monteagudo-Lerma, S. Valdueza-Felip, A. Núñez-Cascajero, M. González-Herráez, E. Monroy, and F.B. Naranjo, "Two-step method for the deposition of AlN by radio frequency sputtering", *Thin Solid Films* vol. 545, pp. 149–153, 2013.

[12] L. Monteagudo-Lerma, '*Morphology and arrangement of InN nanocolumns deposited by radio-frequency sputtering: effect of the buffer layer*', to be published (2015).

[13] R.G. Hunsperger, *Integrated optics: theory and technology*. 4th edition, 1984, pp. 87–89.

[14] A.C. Turner-Foster, M.A. Foster, J.S. Levy, C.B. Poitras, R. Salem, A.L. Gaeta, and M. Lipson, "Ultrashort free-carrier lifetime in low-loss silicon nanowaveguides", *Opt. Express* vol. 18, no. 4, pp. 3582–3591, 2010.

[15] K. Wang, J. Zhou, L. Yuan, Y. Tao, J. Chen, P. Lu, and Z.L. Wang, "Anisotropic third-order optical nonlinearity of a single ZnO micro/nanowire", *Nano Lett.* vol. 12, no. 2, pp. 833–838, 2012.

[16] D. Vignaud, J.F. Lampin, and F. Mollot, "Two-photon absorption in InP substrates in the 1.55 µm range", *Appl. Phys. Lett.* vol. 85, no. 2, pp. 239–241, 2004.

[17] M. Dinu, F. Quochi, and H. Garcia, "Third-order nonlinearities in silicon at telecom wavelengths", *Appl. Phys. Lett.* vol. 82, no. 18, pp. 2954–2956, 2003.